Calculations of superconducting properties in yttrium and calcium under high pressure

Shi Lei,[1] D. A. Papaconstantopoulos,[1,2] and Michael J. Mehl[2]
[1]*Department of Computational and Data Sciences, George Mason University, Fairfax, Virginia 22030, USA*
[2]*Center for Computational Materials Science, Naval Research Laboratory, Washington DC 20375, USA*
(Received 7 September 2006; revised manuscript received 16 November 2006; published 25 January 2007)

We have used first-principles electronic structure calculations to generate the bulk modulus as a function of volume as well as the densities of states and scattering phase shifts at the Fermi level. These quantities were used in conjunction with the rigid-muffin-tin theory of Gaspari and Gyorffy and the McMillan theory to determine the electron-phonon coupling and the superconducting transition temperature for yttrium and calcium under high pressures. Our results provide a good interpretation of the measured increase of T_c in these metals.

DOI: 10.1103/PhysRevB.75.024512 PACS number(s): 74.62.Fj, 74.10.+v, 61.66.Bi

I. INTRODUCTION

In a recent paper Hamlin *et al.*[1] reported diamond anvil experiments in yttrium that show superconductivity under hydrostatic pressure, with a linear increase from T_c=3.5 K at 30 GPa to 17 K at 89 GPa. Earlier x-ray diffraction measurements by Grosshans and Holzapfel[2] suggested a crystal structure sequence hcp-αSm-dhcp-trigonal in the pressure range, with the transitions occurring at 15, 32, and 45 GPa, respectively. It is not clear whether the fcc lattice appears between double hcp (dhcp) and trigonal as it does for a few of the rare-earth metals. A theoretical prediction that Y transforms to the bcc structure at 280 GPa has been made by Melsen *et al.*[3] In addition to yttrium, calcium has also been reported[4] to superconduct at T_c=15 K at pressures of 150 GPa in the simple cubic lattice and at T_c=25 K at 161 GPa.[5] In this work we seek to explain the pressure-dependent superconducting behavior of these elements by using total-energy and electronic band-structure results from first-principles calculations as input to the rigid-muffin-tin approximation (RMTA) developed by Gaspari and Gyorffy.[6,7] We performed general-potential linearized augmented-plane-wave[8] (LAPW) total-energy[9] calculations to determine the relationship between total energy, volume, and pressure for the above crystal structures of Y and Ca. For yttrium we placed the 4*s* and 4*p* states in the semicore, representing them by local orbitals inside the muffin tin,[10] while for calcium we used semicore orbitals for the 3*s* and 3*p* states. We found the best representation of the structural behavior of calcium was obtained using a generalized gradient approximation (GGA),[11] while for yttrium we used the local density approximation (LDA) from the same reference. We made these choices of density functionals in order to ensure that the predicted equilibrium volume of the ground-state structure is in agreement with experiment. For calcium, the LDA equilibrium lattice constant is approximately 4% smaller than experiment,[12] while we find that the GGA equilibrium lattice constant is within 1% of experiment. We thus use the GGA to describe calcium. The LDA equilibrium lattice constant for yttrium is within 1% of experiment; hence, we use the LDA for yttrium.

In Fig. 1 we show the total energy of Y with respect to the hcp lattice as a function of volume and pressure. From this graph and the corresponding calculation of the enthalpy the LDA predicts that the transition from the hcp structure to αSm occurs at −3 GPa; i.e., the ground state of yttrium is αSm, in conflict with experiment. The LDA does predict the correct sequence of phase transitions, with the αSm-dhcp transition at 3 GPa, rather than the 30 GPA found by experiment.[2]

It is significant that at pressures very near 89 GPa, where the maximum T_c was found, the fcc lattice has its minimum energy relative to the hcp structure. However, as noted by Yin and co-workers,[13] at these pressures the fcc structure is unstable with respect to distortions related to the transverse phonons along the [111] direction near the Brillouin zone boundary. We approximate this instability by using a frozen-phonon representation of the L_3^- phonon, minimizing the energy as a function of the displacement of the basis vectors from their positions on the fcc lattice. We find that this distorted structure has a lower energy than the cubic fcc phase for all volumes where the fcc structure has a lower energy than either the αSm or the dhcp structure. This transition

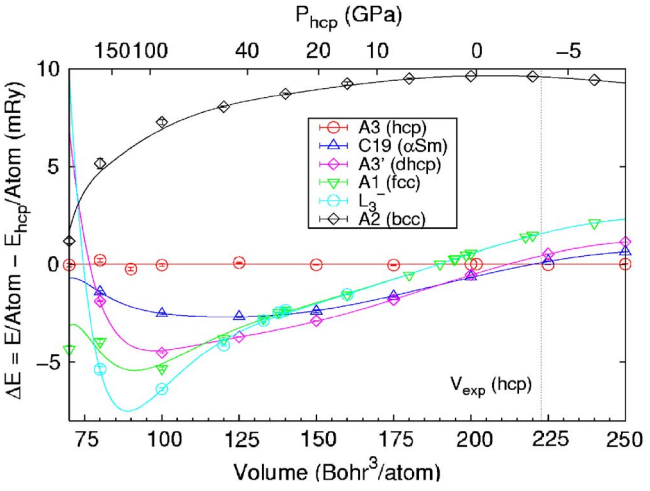

FIG. 1. (Color online) Yttrium total energy relative to a sixth-order Birch fit to the hcp structure. The displacement of the hcp points from the line shows the error in the fit. The pressure scale is the pressure of the hcp structure determined from the fit as a function of the corresponding cell volume. The L_3^- structure is explained in the text.

starts at approximately 40 GPa, close to the experimental transition at 45 GPa.[2] Since the L_3^- structure yields only an upper bound on the energy of all possible distortions of the fcc lattice, the calculations predict that the cubic fcc structure of yttrium will never be seen under hydrostatic pressure.

Using our band-structure results we proceed with a first-principles calculation of the electron-phonon coupling constant λ and the superconducting transition temperature T_c. We take the McMillan approach[7] and write

$$\lambda = \frac{\eta}{M\langle\omega^2\rangle} = \frac{N(\varepsilon_f)\langle I^2\rangle}{M\langle\omega^2\rangle}, \tag{1}$$

where $N(\varepsilon_f)$ is the density of states per spin and $\langle I^2\rangle$ is the electron-ion matrix element.

We calculate the numerator η, known as the Hopfield parameter, within the RMTA. The matrix element $\langle I^2\rangle$, derived from multiple-scattering theory, is given by the formula

$$\langle I^2\rangle = \frac{\epsilon_F}{\pi^2 N^2(\epsilon_F)} \sum_l \frac{2(l+1)\sin^2(\delta_{l+1}-\delta_l)N_l N_{l+1}}{N_l^{(1)} N_{l+1}^{(1)}}. \tag{2}$$

The RMTA formula for η requires accurate calculations of the total (N) and angular momentum components (N_l) of the density of states at the Fermi level; the scattering phase shifts (δ_l), which are calculated from the radial wave functions u_l, spherical Bessel functions j_l and Neumann functions n_l at the muffin-tin radius R_s from the well-known formula[15]

$$\frac{u_l'(r,\varepsilon_F)}{u_l(r,\varepsilon_F)} = \left.\frac{j_l'(kr) - n_l'(kr)\tan\delta_l}{j_l(kr) - n_l(kr)\tan\delta_l}\right|_{r=R_s}, \tag{3}$$

and the free-scatterer density of states,

$$N_l^{(1)} = \frac{\sqrt{\varepsilon_F}}{\pi}(2l+1)\int_0^{R_s} u_l^2(r,\varepsilon_F) r^2 dr. \tag{4}$$

Since Eq. (2) is based on scattering theory, it should be applied using touching muffin-tin spheres, as the excess interstitial volume in the case of nontouching spheres introduces errors. In our recent papers[16] on superconductivity of the alkali metals we have demonstrated that Eq. (2) has been misused in the past and if applied properly is sufficiently accurate to understand the pressure variation of T_c. For the determination of the denominator of Eq. (1) we approximate

$$\langle\omega^2\rangle = \frac{1}{2}\Theta_D^2 \tag{5}$$

and obtain the Debye temperature Θ_D using the formula given by Moruzzi *et al.*:[17]

$$\Theta_D = 131.6\sqrt{\frac{r_0 B}{M}}, \tag{6}$$

where B is the bulk modulus (in GPa), r_0 is the Wigner-Seitz radius in Bohr units, and M is the atomic mass. The resulting average phonon frequency and its variation with volume enter both in the calculation of λ and in the prefactor of the McMillan equation for T_c:

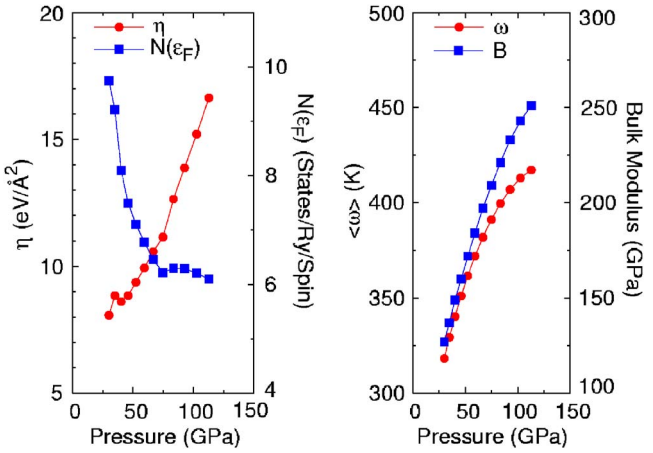

FIG. 2. (Color online) η, $N(\varepsilon_f)$, bulk modulus, and $\langle\omega^2\rangle$ of fcc yttrium, derived from first-principles LAPW calculations.

$$T_c = \frac{\langle\omega\rangle}{1.2}\exp\left[\frac{-1.04(1+\lambda)}{\lambda-\mu^*(1+0.62\lambda)}\right]. \tag{7}$$

This approach is appealing for its simplicity, and it turns out to be fairly accurate, leading to results that are in agreement with experiment. It should also be noted that this approach is very well converged with respect to the k-point integration over the Brillouin zone, a serious issue in calculations using linear response theory.[18]

II. RESULTS

A. Yttrium

The different crystal structures of Y starting from hcp down to αSm and dhcp are all closed-packed structures, so in presenting our results for the parameters controlling superconductivity we will make the simplifying assumption of performing the RMTA calculations in the fcc lattice. This assumption was also made by Yin *et al.*,[13] and it is justified on the basis that the unstable L_3^- transverse phonon distortion results in a displacement of only 0.06 a.u. perpendicular to the [111] direction. In the left panel of Fig. 2 we show the parameter η and the total density of states $N(\varepsilon_f)$ per spin at the Fermi level ε_f, as a function of pressure. We note that although $N(\varepsilon_f)$ decreases with pressure, η increases. This is clearly due to a rapid increase of the electron-ion matrix element $\langle I^2\rangle$ that multiplies $N(\varepsilon_f)$ to get η. The increase of $\langle I^2\rangle$ comes from the increase of the d character of states at ε_f. In the right panel the pressure variation of the bulk modulus is shown together with $\langle\omega\rangle$. Since we have taken $\langle\omega\rangle$ to be roughly proportional to B, they both show a similar increase with pressure, although the r_0 factor in Eq. (6) somewhat dampens the increase of $\langle\omega\rangle$. We then proceed to calculate λ, shown in the left panel of Fig. 3. We see that λ is about constant at lower pressures but then increases rapidly at the higher pressures. Finally, in the right panel of Fig. 3 we show the variation of T_c with pressure found using the McMillan equation. It is evident that the T_c results are strongly dependent on the value of μ^*. For $\mu^*=0.13$, although we reproduce the trend of the increase of T_c shown in the experiments of Hamlin *et al.*,[1] there is no quantitative agreement. We

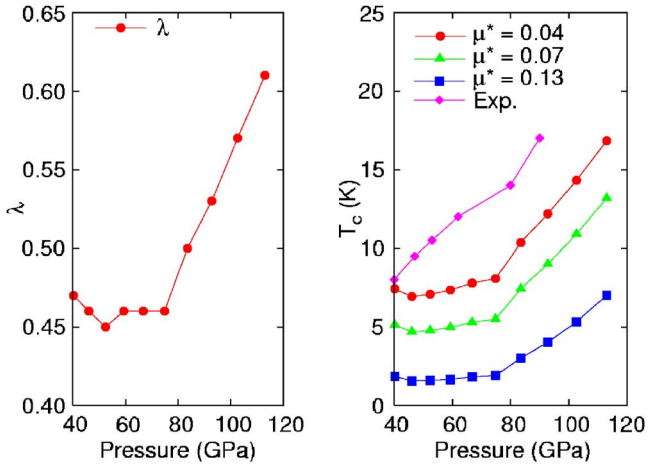

FIG. 3. (Color online) λ and T_c of fcc yttrium. Experimental data are from Hamlin *et al.* (Ref. 1).

believe that it is not realistic to expect good agreement with experiment until we have an accurate determination of μ^*; however, we note that $\mu^*=0.04$ gives good agreement with experiment. How significant this is should be decided if a first-principles determination of μ^* can be made. Our results for Y are also summarized in Table I where we list all quantities entering the McMillan approach.

To further test the validity of pursuing these calculations in the undistorted fcc lattice, we actually performed a calculation of the coupling constant λ for the distorted L_3^- phonon and found values in the range of 0.5–0.7, which give similar values for T_c as in the fcc within the uncertainties of the choice of μ^*. We have also performed calculations for the bcc structure which is predicted to occur at pressures well over 200 GPa, in agreement with Melsen *et al.*[3] Our results for both the L_3^- and bcc structures are also shown in Table I, indicating that superconductivity is possible in the bcc lattice as well.

B. Calcium

Using the same methodology we evaluated the electron-phonon coupling and T_c in Ca. We have previously shown[19] that under pressure fcc Ca transforms into an insulator and under further compression becomes a metal again upon

TABLE I. The input quantities necessary to compute T_c via the McMillan approach (Ref. 14) (1)–(7), along with the computed value of T_c, for fcc and bcc yttrium. The experimental values of T_c are from a quadratic curve fit to the data in Hamlin *et al.* (Ref. 1).

Phase	V/V_0	P (GPa)	B (GPa)	$N(\varepsilon_F)$ (st/Ry/sp)	η (eV/Å^2)	λ	ω (K)	T_c (K)	T_c (K)	T_c (K)	T_c (K)
μ^*								0.04	0.07	0.13	(Expt.[a])
bcc	0.33	332	1083	6.11	30.26	0.36	734		3	0.5	
bcc	0.35	274	903	6.89	30.30	0.42	676		7	2	
bcc	0.37	227	754	8.73	35.13	0.57	624		17	8	
bcc	0.39	188	632	10.65	36.59	0.70	577		25	15	
fcc	0.45	113	251	6.10	16.63	0.61	417	17	13	7	20
fcc	0.47	103	243	6.21	15.20	0.57	413	14	11	5	19
fcc	0.49	93	233	6.29	13.87	0.53	407	12	9	4	11
fcc	0.51	84	221	6.30	12.64	0.50	400	10	7	3	15
fcc	0.53	75	209	6.22	11.15	0.46	391	8	6	2	14
fcc	0.56	67	197	6.46	10.58	0.46	382	8	5	2	13
fcc	0.58	59	184	6.78	9.94	0.46	372	7	5	2	11
fcc	0.60	52	172	7.10	9.37	0.45	362	7	5	2	10
fcc	0.63	46	160	7.49	8.85	0.46	351	7	5	2	9
fcc	0.65	40	149	8.09	8.61	0.47	340	7	5	2	8
fcc	0.67	35	137	9.21	8.85	0.52	329	9	7	3	7
fcc	0.70	30	127	9.74	8.07	0.51	318	8	6	2	6
L_3^-	0.184	14900	282	10.24	17.65	0.75	386	23	19	12	
L_3^-	0.230	8740	260	11.85	12.98	0.56	385	13	10	5	
L_3^-	0.276	5013	200	13.05	8.94	0.47	348	7	5	2	
L_3^-	0.306	3431	142	15.33	7.31	0.52	298	9	6	3	
L_3^-	0.318	2946	115	15.56	6.94	0.61	270	11	8	4	
L_3^-	0.322	2768	104	15.56	6.49	0.63	257	11	9	5	

[a]Reference 1.

transformation to the bcc structure. We have now performed new total-energy calculations by the LAPW method, as shown in Fig. 4. We found structural transitions from fcc to bcc at 10 GPa, from bcc to simple cubic at 43.5 GPa, and from simple cubic to hcp at 95 GPa. The comparable experimental values are[20] 20, 32, and 40 GPa, though the last transition is to an unknown phase. As with yttrium, density functional theory (DFT) calculations, in this case using a GGA functional, correctly describe the ordering of the transitions, but not the correct transition pressure.

The interesting behavior in the hcp energy at volumes below 100 bohr^3/atom is caused by the formation of a double well in the energy as a function of c/a. One of the minima of this well is near the ideal value $\sqrt{8/3}$, while the other well begins near the ideal value and then decreases to about 1.3 at $V=60$ bohr^3. The dip in the $E_{hcp}-E_{fcc}$ curve occurs when this "small c/a" structure has the lowest energy. For volumes below 60 bohr^3 the near-ideal hcp lattice again has the lower energy. In the small c/a structure the Fermi level is at a minimum of the electronic density of states, and so in this

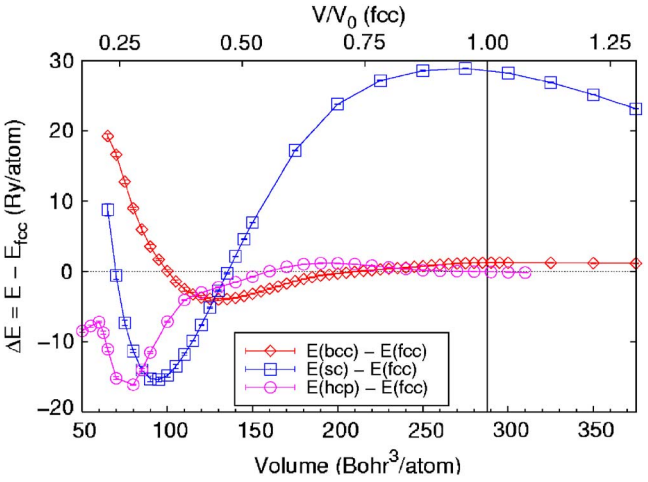

FIG. 4. (Color online) Calcium total energy with respect to the energy in the fcc phase for the bcc, simple cubic, and hcp phases. The transition pressure between each phase is discussed in the text, as is the unusual shape of the hcp curve at high pressure.

TABLE II. The input quantities necessary to compute T_c via the McMillan approach (Ref. 14) (1)–(7), along with the computed value of T_c, for simple cubic calcium. All calculations for T_c use $\mu^*=0.13$. The experimental values of T_c are taken from a quadratic fit to the data of Okada *et al.* (Ref. 4). The pressure and bulk modulus are given in GPa, the DOS expressed as states/Ry/spin, η has units of eV/Å^2, and ω and T_c are in kelvin.

Phase	V/V_0	P	B	$N(\varepsilon_F)$	η	λ	ω	T_c	Expt.[a]
sc	0.220	182	405	4.98	18.75	3.02	296	51	24
sc	0.230	155	334	5.46	19.20	3.75	269	50	16
sc	0.250	134	286	5.96	19.92	4.53	249	50	11
sc	0.270	116	253	6.78	21.45	5.52	234	49	8
sc	0.285	102	227	4.67	10.23	2.93	222	38	5
sc	0.300	90	206	4.11	7.07	2.23	211	31	4
sc	0.320	79	188	3.76	5.24	1.82	202	25	3
sc	0.335	70	172	3.46	3.98	1.51	193	20	2
sc	0.350	62	157	3.35	3.32	1.38	184	17	2
sc	0.370	55	144	3.05	2.50	1.13	176	13	2
sc	0.385	48	131	2.81	2.09	1.03	169	11	2
sc	0.400	43	120	2.17	1.55	0.84	161	7	
sc	0.420	38	110	2.12	1.29	0.76	154	5	
sc	0.440	34	101	1.97	1.10	0.71	148	4	
sc	0.450	31	92	1.80	0.87	0.62	141	3	
bcc	0.25	141	195	6.78	18.74	1.20	468	37	12
bcc	0.28	119	194	5.34	15.21	0.95	476	26	8
bcc	0.31	99	182	5.53	11.44	0.73	469	14	4
bcc	0.35	81	163	5.22	7.99	0.55	452	5	3
bcc	0.38	65	145	4.70	5.24	0.39	434	0.7	2
bcc	0.42	52	126	4.80	3.89	0.32	411	0.1	
bcc	0.47	40	107	4.77	2.91	0.28	385	0.01	
bcc	0.51	31	90	4.78	2.09	0.23	358	0	
bcc	0.56	24	75	4.91	1.54	0.20	332	0	
bcc	0.61	18	63	5.13	1.12	0.17	308	0	

[a]Reference 4.

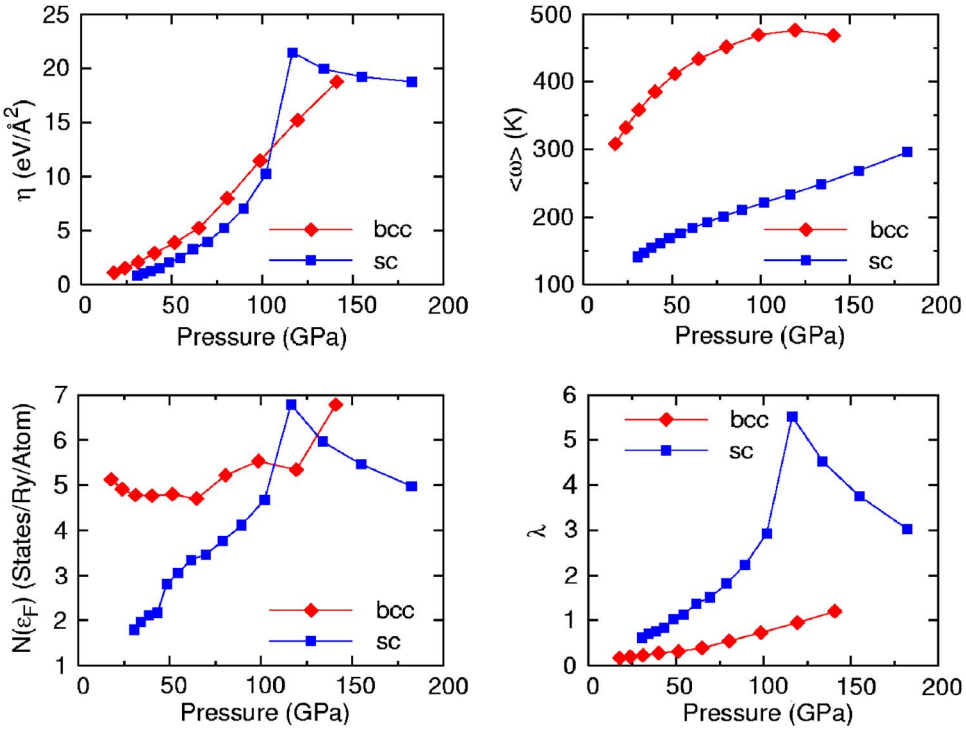

FIG. 5. (Color online) η, $\langle\omega\rangle$, $N(\varepsilon_F)$, and λ for bcc (red diamonds) and simple cubic (blue squares) calcium.

region Ca will have a very low T_c.

Using these results, we noted that the pressure range covered by the experiment is in the region of the bcc and sc structures. We accordingly computed the quantities needed for the RMTA for these structures, summarizing our work in Table II and in Fig. 5. As is shown in Fig. 5 for sc Ca both $N(\varepsilon_F)$ and η increase monotonically with increasing pressure. We note that this behavior is different from Y where $N(\varepsilon_F)$ decreases under pressure.

The increase of $N(\varepsilon_F)$ in Ca is contrary to our usual expectation that the broadening of the DOS under increasing pressure would result in a decrease in the DOS at any given energy, especially at the Fermi level. In Fig. 6 we plot the total DOS for Ca in the simple cubic structure at pressures of 30, 61, 153, and 189 GPa. At the lower two pressures ε_F falls in the middle of a pseudogap which keeps $N(\varepsilon_F)$ low. However, at the higher pressures ε_F moves away from this gap and into the Ca d bands, increasing $N(\varepsilon_F)$ by a factor of 2.

Also in Fig. 5 we show the expected increase of $\langle\omega\rangle$ with increasing pressure and the resulting pressure dependence of λ. For pressures of over 100 GPa λ reaches unusually large values, and as a result the predicted value of T_c, shown in Fig. 7, seriously overestimates the experimental values. The large values for λ are achieved because of the rapid increase of η at pressures above 100 GPa, which can be traced to the rise of the matrix element $\langle T^2\rangle$, as shown in Fig. 8. Often it is argued that spin fluctuations have a limiting effect on T_c. In that case a λ_{spin} is introduced into the McMillan equation, which in our case would reduce our calculated T_c by about

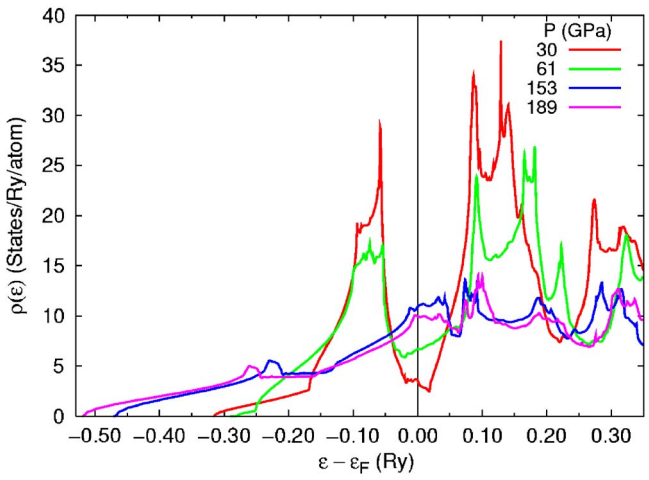

FIG. 6. (Color online) Density of states for simple cubic calcium at several pressures. The Fermi level is set to zero for each pressure.

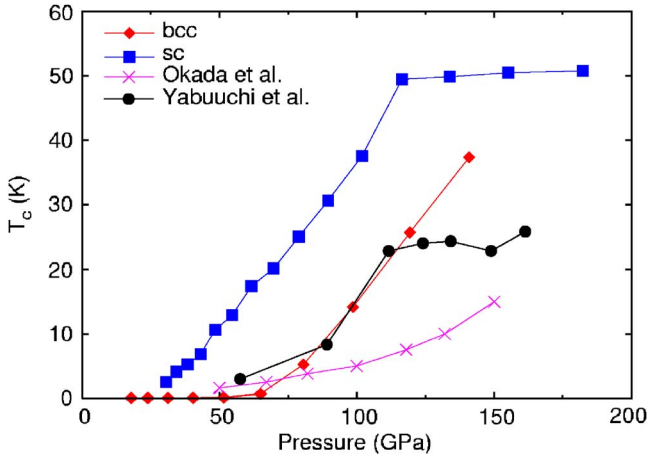

FIG. 7. (Color online) Prediction of T_c for bcc (red diamonds) and simple cubic (blue squares) calcium from Eq. (7), compared to the experimental values of Okada *et al.* (Ref. 4) (mauve crosses) and Yabuuchi *et al.* (Ref. 5) (black circles).

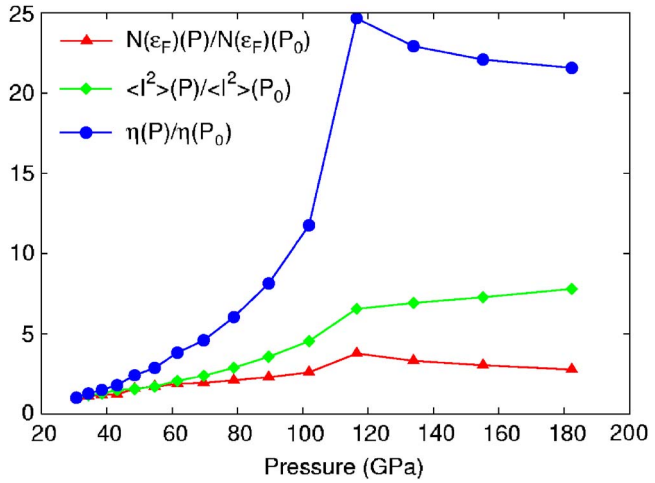

FIG. 8. (Color online) Pressure dependence of the electronic density of states at the Fermi level $N(\varepsilon_F)$ (red circles), $\langle I^2\rangle$ Eq. (2) (green triangles), and η (blue diamonds) for calcium. Each quantity is plotted as a ratio of its value at the current pressure to its value at the reference pressure, P_0=30 GPa.

4 K for λ_{spin}=0.1-0.2. We have calculated the Stoner parameter from our band-structure results and the Vosko-Perdew[21] theory and found that at high pressures the Stoner I ranges between 0.012 and 0.014 Ry. Using our results for $N(\varepsilon_F)$ we find a Stoner criterion of about 0.1. This small value justifies neglecting spin fluctuations and the λ_{spin} parameter.

A close inspection of Tables I and II reveals that the large values of λ obtained for high pressures (small volumes) in Ca are due to the small values of $\langle\omega\rangle$ at these volumes. On the other hand, at the small volumes in Y we find that $\langle\omega\rangle$ is more than twice as large as in Ca, causing λ to become much smaller.

The large increase in η at small volumes for Ca, shown in Fig. 8, can be explained by noting that $N(\varepsilon_F)$ retains modest values, while $\langle I^2\rangle$ increases significantly, causing a dramatic increase in the value of η. Equation (2) shows that $\langle I^2\rangle$ depends on both the phase shift factor $\sin^2(\delta_{l+1}-\delta_l)$, plotted in

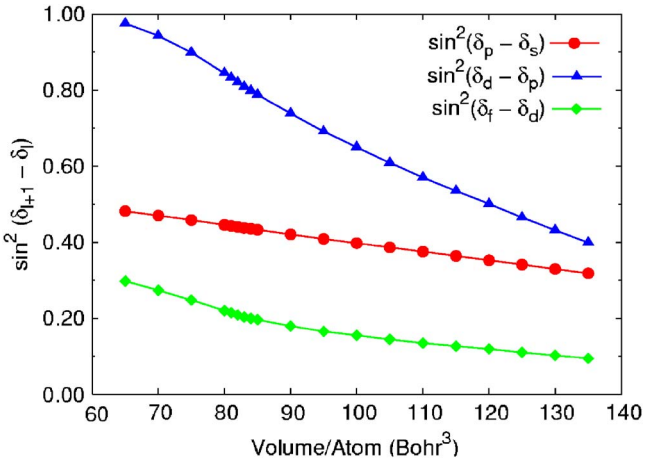

FIG. 9. (Color online) The phase shift factor $\sin^2(\delta_{l+1}-\delta_l)$ from Eq. (2) for l=0 (red circles), l=1 (blue triangles), and l=2 (green diamonds).

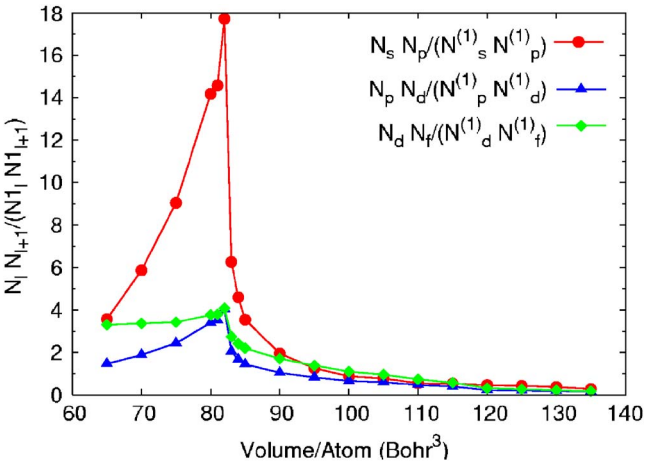

FIG. 10. (Color online) The angular-momentum-decomposed and free-scatterer-decomposed DOS $(N_lN_{l+1})/(N_l^{(1)}N_{l+1}^{(1)})$ from Eq. (2) for l=0 (red circles), l=1 (blue triangles), and l=2 (green diamonds).

Fig. 9, and the ratio $(N_lN_{l+1})/(N_l^{(1)}N_{l+1}^{(1)})$, plotted in Fig. 10.

Of course the calculated T_c strongly depends on our chosen value of μ^*=0.13. We note that raising the value of μ^* to 0.20 reduces T_c by roughly 20%. In Table II we also list results for bcc Ca. In this case λ is much smaller and hence the calculated T_c is also smaller. It is not clear whether the experimental measurements correspond to the sc or bcc lattice.

III. CONCLUSIONS

On the basis of band-structure calculations, the RMTA, and the McMillan theory of superconductivity, we have accounted for the superconducting behavior of Y and Ca under pressure. Our approach for calculating the electron-phonon coupling differs from recent work[13] on Y using linear response theory, which leads to unusually high value of λ close to 3.0 even at the modest pressure of 42 GPa. It is possible that this value of λ can be reduced by performing the calculations using a denser Brillouin-zone sampling. Our values of λ are less than 1.0 even at pressures above 100 GPa, which, within the uncertainty of the value of the Coulomb pseudopotential μ^*, gives values of T_c near experiment. On the other hand for Ca we obtain large values of λ and consequently overestimate T_c. In any case the increase of T_c with pressure seen in the experiments for both these metals is unambiguously demonstrated by these calculations in terms of an electron-phonon mechanism.

The problem with μ^* has been eliminated in the recently proposed theory of superconductivity by Profeta *et al.*[22] It would be helpful if μ^* could be extracted or inferred from this theory. In addition, it would be extremely valuable for the determination of λ if measurements of the Sommerfeld coefficient γ could be made under high pressure.

ACKNOWLEDGMENT

This work was supported by the U.S. Office of Naval Research. We wish to thank W. E. Pickett for useful suggestions.

[1] J. J. Hamlin, V. G. Tissen, and J. S. Schilling, Phys. Rev. B **73**, 094522 (2006).
[2] W. A. Grosshans and W. B. Holzapfel, Phys. Rev. B **45**, 5171 (1992).
[3] J. Melsen, J. M. Wills, B. Johansson, and O. Eriksson, Phys. Rev. B **48**, 15574 (1993).
[4] S. Okada, K. Shimizu, T. Kobayashi, K. Amaya, and S. Endo, J. Phys. Soc. Jpn. **65**, 1924 (1996).
[5] T. Yabuuchi, T. Matsuoka, Y. Nakamoto, and K. Shimizu, J. Phys. Soc. Jpn. **75**, 083703 (2006).
[6] G. D. Gaspari and B. L. Gyorffy, Phys. Rev. Lett. **28**, 801 (1972).
[7] W. H. Butler, J. J. Olson, J. S. Faulkner, and B. L. Gyorffy, Phys. Rev. B **14**, 3823 (1976).
[8] O. K. Andersen, Phys. Rev. B **12**, 3060 (1975).
[9] S.-H. Wei and H. Krakauer, Phys. Rev. Lett. **55**, 1200 (1985).
[10] D. Singh, Phys. Rev. B **43**, 6388 (1991).
[11] J. P. Perdew, J. A. Chevary, S. H. Vosko, K. A. Jackson, M. R. Pederson, D. J. Singh, and C. Fiolhais, Phys. Rev. B **46**, 6671 (1992).
[12] M. J. Mehl and D. A. Papaconstantopoulos, Phys. Rev. B **54**, 4519 (1996).
[13] Z. P. Yin, S. Y. Savrasov, and W. E. Pickett, Phys. Rev. B **74**, 094519 (2006).
[14] W. L. McMillan, Phys. Rev. **167**, 331 (1968).
[15] J. M. Ziman, *Principles of the Theory of Solids* (Cambridge University Press, Cambridge, England, 1964), Chap. 3.
[16] L. Shi, D. A. Papaconstantopoulos, and M. J. Mehl, Solid State Commun. **127**, 13 (2003); L. Shi and D. A. Papaconstantopoulos, Phys. Rev. B **73**, 184516 (2006).
[17] V. L. Moruzzi, J. F. Janak, and K. Schwarz, Phys. Rev. B **37**, 790 (1988).
[18] D. Kasinathan, K. Koepernik, J. Junes, H. Rosner, and W. E. Pickett, Physica C (to be published).
[19] G. M. Wang, D. A. Papaconstantopoulos, and E. Blaisten-Barojas, J. Phys. Chem. Solids **64**, 185–192 (2003).
[20] H. Olijnyk and W. B. Holzapfel, Phys. Lett. **100A**, 191 (1984).
[21] S. H. Vosko and J. P. Perdew, Can. J. Phys. **53**, 1385 (1975).
[22] G. Profeta, C. Franchini, N. N. Lathiotakis, A. Floris, A. Sanna, M. A. L. Marques, M. Lüders, S. Massidda, E. K. U. Gross, and A. Continenza, Phys. Rev. Lett. **96**, 047003 (2006).